

# Building Solid-State Batteries: Insights from Swiss Research Labs

Kostiانتyn V. Kravchyk<sup>\*a,b</sup>, Corsin Battaglia<sup>a,c,d</sup>, Valerie Siller<sup>e</sup>, Barthélémy Lelotte<sup>e</sup>, Mario El Kazzi<sup>e</sup>, Jędrzej Morzy<sup>a</sup>, Moritz Futscher<sup>a</sup>, Yaroslav Romanyuk<sup>a</sup>, Michael Stalder<sup>f</sup>, Axel Fuerst<sup>f</sup> and Maksym V. Kovalenko<sup>\*a,b</sup>



**Abstract:** This review article delves into the growing field of solid-state batteries as a compelling alternative to conventional lithium-ion batteries. The article surveys ongoing research efforts at renowned Swiss institutions such as ETH Zurich, Empa, Paul Scherrer Institute, and Berner Fachhochschule covering various aspects, from a fundamental understanding of battery interfaces to practical issues of solid-state battery fabrication, their design, and production. The article then outlines the prospects of solid-state batteries, emphasizing the imperative practical challenges that remain to be overcome and highlighting Swiss research groups' efforts and research directions in this field.

**Keywords:** Li metal anode · Solid-state batteries · Solid-state electrolyte



**Maksym V. Kovalenko** obtained an MS Chemistry (2004) from Chernivtsi National University (Ukraine) and a PhD (2007) from JKU Linz (Austria). After postdoctoral training (2008–2011, at University of Chicago, USA), he moved to Switzerland, where he is currently a full professor at ETH Zurich (Institute for Inorganic Chemistry) and Empa. His research encompasses bulk semiconductors for hard radiation

detection, synthesis, surface chemistry, spectroscopy and self-assembly of quantum dots, as well as novel materials for rechargeable batteries. He co-authored *ca.* 400 articles and 14 patents.



**Kostiانتyn V. Kravchyk** obtained his PhD degree from Vernadsky Institute of General and Inorganic Chemistry of the Ukrainian National Academy of Sciences in 2009. Then, he completed his postdoctoral research at the University of Le Mans (France), the University of Nantes (France), and ETH Zurich and Empa (Swiss Federal Laboratories for Materials Science and Technology). He now works as a senior

scientist at Empa in the Functional Inorganic Materials group of Prof. Maksym Kovalenko. His research interests include all-solid-state Li-ion batteries, novel concepts for electrochemical energy storage, and novel materials for Li-ion and post-Li-ion batteries.



**Corsin Battaglia** is directing the laboratory of Materials for Energy Conversion at Empa, the Swiss Federal Laboratories of Materials Science and is an Adjunct Professor of Electrical Engineering at ETH Zurich, Department of Information Technology and Electrical Engineering and an Adjunct Professor of Materials Science at EPFL, School of Engineering, Institute of Materials. His current research focuses

on sustainable next-generation lithium-ion batteries, post-lithium-ion batteries, and the electrochemical conversion of CO<sub>2</sub> to synthetic fuels. After receiving his PhD in Physics from the Université de Neuchâtel, he was a postdoctoral researcher at EPFL, the University of California Berkeley, and Lawrence Berkeley National Laboratories, before joining Empa in 2014. He is co-author of more than 150 peer-reviewed scientific publications and 7 patent applications.



Mario El Kazzi, Valerie Siller, Barthélémy Lelotte

**Dr. Mario El Kazzi** is currently the head of 'Battery Materials and Diagnostics' (BMD) group in the Electrochemistry Laboratory, at Paul Scherrer Institute (PSI), Switzerland. He obtained his PhD

\*Correspondence: Dr. K. V. Kravchyk, E-mail: Kostiانتyn.Kravchyk@empa.ch and Prof. M. V. Kovalenko, E-mail: mvkovalenko@ethz.ch

<sup>a</sup>Empa – Swiss Federal Laboratories for Materials Science and Technology, Überlandstrasse 129, CH-8600 Dübendorf, Switzerland; <sup>b</sup>Laboratory of Inorganic Chemistry, Department of Chemistry and Applied Biosciences, ETH Zürich, Vladimir-Prelog-Weg 1, CH-8093 Zürich, Switzerland; <sup>c</sup>Department of Information Technology and Electrical Engineering, ETH Zurich, Gloriastrasse 35, CH-8092 Zurich, Switzerland; <sup>d</sup>Institute of Materials, School of Engineering, EPFL, Station 17, CH-1015 Lausanne, Switzerland; <sup>e</sup>Electrochemistry Laboratory, Paul Scherrer Institute, CH-5232 Villigen PSI – Switzerland; <sup>f</sup>Institute for Intelligent Industrial Systems I3S, Berner Fachhochschule, Pestalozzistrasse 20, CH-3400 Burgdorf, Switzerland.

from Ecole centrale de Lyon – Institute of Nanotechnologies of Lyon (INL), France in 2008. He has had numerous post-doctoral positions, namely, SOLEIL synchrotron at TEMPO beamline (2008–2010) and IBM Zurich Research Laboratory (2010–2013) before joining PSI. Currently Dr. Mario El Kazzi's research covers areas related to electrochemistry of lithium/sodium-ion liquid and solid-state type batteries with a focus on advanced surface and bulk *operando* techniques using laboratory and synchrotron scale facilities.

**Dr. Valerie Siller** is currently a Postdoc in the BMD group, in the Electrochemistry Laboratory, at Paul Scherrer Institute (PSI), Switzerland, focusing on the *operando* characterization of all-solid-state battery interfaces.

**Barthélémy Lelotte** is a PhD student in the BMD group in the Electrochemistry Laboratory, at Paul Scherrer Institute (PSI), Switzerland, working on the interface characterization and optimization of sulfide-based SSBs employing high voltage cathode materials.



**Dr. Jędrzej Morzy, Dr. Moritz Futscher, and Dr. Yaroslav Romanyuk** are members of the 'Thin-film batteries' group in the Laboratory for Thin Films and Photovoltaics at Empa (<https://www.empa.ch/web/s207/thin-film-batteries>). The group has been developing thin-film micro-batteries since 2013 using the glovebox-integrated fabrication line that allows manufacturing and electrochemical characterization of battery devices. The focus is on vacuum deposition methods (sputtering, evaporation, ALD) of thin films and coatings, as well as advanced analytics with electrochemical characterisation, electron microscopies (FIB-SEM, TEM), XPS, and TOF-SIMS to study interfacial phenomena and degradation mechanisms. The group also demonstrated successful technology transfer to the Empa spin-off *BTRY*.



**Prof. Dr. Axel Fuerst** is the dean of the faculty of Mechanical Engineering at the Bern University of Applied Sciences. He founded a research group on production optimization and battery production. The group is active in many Swiss and EU research projects. Before his carrier in academia he worked for many years in global functions at multinational companies. He received his PhD degree from the University of Kaiserslautern in a sandwich doctorate with Universidade Estadual de Campinas.



**Michael Stalder** is a research team leader at the Institute for Smart Industrial Systems at the Bern University of Applied Sciences and a lecturer for control system engineering at the faculty of Mechanical Engineering. His work is focused on technology development for production process optimization and battery manufacturing. He holds a Master's Degree in Mechanical Engineering from

EPFL (Ecole Polytechnique Fédérale de Lausanne), Switzerland, and has 9 years industrial experience working with Advanced Process Control and Process Optimization solutions.

## 1. Introduction

Lithium-ion batteries (LIBs) have become a leading electrochemical energy storage technology, which demonstrated remarkable progress in volumetric and gravimetric energy densities over the last decade, reaching *ca.* 770 Wh L<sup>-1</sup> and 260 Wh kg<sup>-1</sup>, respectively. Nevertheless, despite these advances, conventional LIBs inevitably approach their energy density limit, prompting the search for alternative energy storage concepts that can overcome the physicochemical limitations of LIBs.<sup>[1]</sup> Solid-state batteries (SSBs) utilizing solid-state electrolytes (SSE) paired with Li metal anodes stand out as a compelling alternative, with the potential to achieve higher energy densities and power densities, motivating an immense academic research effort across the globe<sup>[2–9]</sup> as well as by major industrial players (Samsung, CATL, VW, Toyota, Ford, BMW, and Mercedes-Benz) and smaller companies (Solid Power, QuantumScape, Swiss Clean Battery and EightInks are actively engaged in the development of SSBs).

Given the dynamic advancements in SSB technology and its anticipated global significance, this review article offers insights into ongoing research endeavours in this field. Specifically, it focuses on elucidating the research activities currently underway at Swiss institutions, including ETH Zurich, Empa, Paul Scherrer Institute (PSI), and Berner Fachhochschule. The article starts with a brief overview of SSB principles and key performance indicators, followed by a discussion of research activities conducted by various research groups working on SSBs in Switzerland, such as Functional Inorganic Materials (FIM Lab, ETH Zurich/Empa), Materials for Energy Conversion (MEC Lab, Empa/ETH Zurich/EPFL), Battery Materials and Diagnostics (BMD group, PSI), Thin Films and Photovoltaics (Empa), and Process Optimization in Manufacturing (Berner Fachhochschule). Finally, the article provides an overview of the prospects for SSBs and emphasizes directions for further research and practical obstacles that remain to be explored.

## 2. The Working Principle of SSB and Key Performance Metrics

In short, the schematics of SSBs closely resemble that of LIBs (Fig. 1), with a key distinction: the liquid electrolyte, acting as a transport medium for lithium ions between the positive and negative electrodes, is replaced by its solid counterpart. During the charging process, the positive electrode undergoes oxidation, releasing Li ions that migrate through the solid electrolyte to the negative electrode, where they are reduced to form metallic lithium. The opposite processes occur during discharge.

Notably, substituting the liquid electrolyte with a solid counterpart does not enhance the battery's energy density. In fact, its gravimetric energy density may even decrease due to the higher density of solid electrolytes compared to liquids. Therefore, integrating solid electrolytes into LIBs becomes compelling only when high charge-storage capacity anodes, such as thin lithium

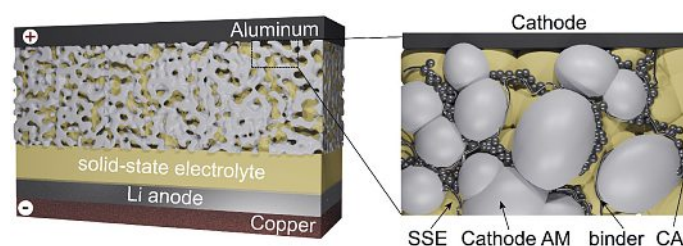


Fig. 1. Schematics of a solid-state Li metal battery. Adapted from ref. [16] Springer Nature.

metal (5–10  $\mu\text{m}$ ), replace conventionally used graphite anodes and when manufacturing bipolar SSB stacks to downsize the packaging. It is also imperative to iterate that the intricate challenge of integrating SSEs into LIBs as a replacement for liquid electrolytes necessitates a simultaneous consideration of multiple crucial performance metrics. These metrics encompass the energy and power density of the targeted SSBs, their long-term stability, cycle and calendar life, safety considerations, and the cost per kWh of energy stored. For a detailed overview of the different families of solid-state electrolytes along with the challenges associated with their employment in SSBs, the reader is referred to some excellent reviews elsewhere.<sup>[10–15]</sup>

## 2.1 The Research Activities in the Functional Inorganic Materials group (Empa/ETHZ)

While SSBs have garnered considerable attention, there remains a lack of consensus within the research community regarding the optimal configuration of SSBs and the choice of SSEs to be used in conjunction with Li metal. For example, when considering solely the Li-metal-based anode aspect of SSBs, there are divergent opinions regarding its design, which ultimately must be addressed:<sup>[17]</sup> (i) the dynamic expansion and shrinkage of Li metal (ranging from 5–25  $\mu\text{m}$  for an area capacity of 1–5  $\text{mAh cm}^{-2}$ ); and (ii) the pertinent challenge of void formation at the Li/solid-state electrolyte interface. As to the latter, it should be noted that experimentally, it has been demonstrated that the formation of voids at the Li/SSE interface occurs while Li is being stripped.<sup>[18,19]</sup> Consequently, this leads to the reduction of the Li/SSE contact area and the increase of the local current densities at the Li/SSE interface during the subsequent Li plating.<sup>[20–22]</sup> The void formation can, therefore, induce Li dendrite formation at much lower current densities than those required for dendrite formation in the unstripped Li/SSE interface.

Initially, it was proposed that the challenges of volume changes and void formation could be addressed by applying pressure at the interface between the SSE and lithium.<sup>[23–26]</sup> However, employing pressure unavoidably introduces non-active components into the battery design, consequently lowering the energy density. Moreover, external stack pressure is regarded as a double-edged sword, as it can accelerate cell failure by subjecting the SSE to heightened mechanical stress, thereby initiating crack propagation.<sup>[14,27]</sup> In this context, a novel scaffold-type design for the anode side of SSBs has recently been extensively investigated by the FIM group (Maksym Kovalenko and Kostiantyn Kravchyk).<sup>[28–31]</sup> This design uses  $\text{Li}_7\text{La}_3\text{Zr}_2\text{O}_{12}$  (LLZO) as the solid-state electrolyte due to its high chemical stability with metallic lithium, high ionic conductivity (up to 1  $\text{mS cm}^{-1}$  at RT), and low electronic conductivity (*ca.*  $10^{-8}$   $\text{S cm}^{-1}$  at RT).<sup>[32]</sup> The scaffold-like architecture of LLZO shows promise in addressing two key challenges: the dynamic volume changes of the Li anode and the formation of voids (Fig. 2a). During Li deposition, the porous structure of LLZO allows for Li storage within its pores, thus mitigating dynamic changes in cell volume. Additionally, the larger surface area of the LLZO/Li interface in the scaffold compared to dense LLZO membranes helps prevent void formation during stripping. Another significant advantage of porous LLZO structures is their potential to reduce the likelihood of Li dendrite formation and voids at the LLZO/Li interface, owing to the larger contact area between Li and LLZO compared to flat LLZO/Li interfaces.

In addition to designing SSEs to support effective Li plating/stripping at the negative electrode, the FIM group has addressed another crucial aspect of practical importance: developing a methodology for large-scale fabrication of porous SSEs in the form of thin LLZO membranes.<sup>[31,33]</sup> As indicated in the recent work<sup>[17]</sup> conducted by the FIM group, employing LLZO SSEs with a thickness of < 100  $\mu\text{m}$  and a porosity of > 20% is essential to achieve a volumetric energy density comparable to conventional Li-ion

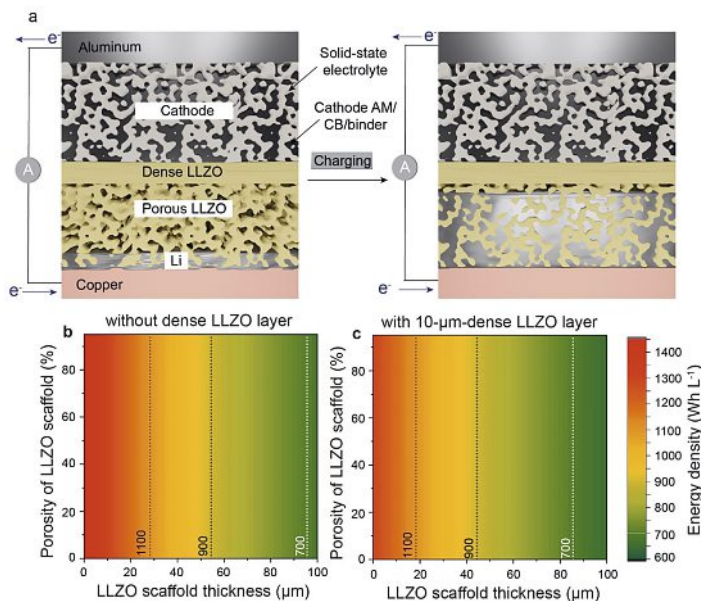


Fig. 2. (a) Schematics of the charging process of Li-garnet solid-state batteries based on dense/porous LLZO membranes. (b, c) Calculated volumetric energy densities of Li-garnet SSBs based on porous (b) and dense/porous (c) LLZO membranes vs the thickness and porosity of the porous LLZO layer. Reproduced with permission ref. [17]. Copyright 2022, The American Chemical Society.

batteries. For instance, in a hypothetical all-solid-state system utilizing LLZO with conventional  $\text{LiCoO}_2$  (LCO) cathode, the employment of LLZO membranes with a thickness of 85  $\mu\text{m}$  and a porosity of > 20%, combined with cathodes of 3.5  $\text{mAh cm}^{-2}$ , is necessary to attain an energy density of 700  $\text{Wh L}^{-1}$  (Fig. 2b). To achieve higher energy densities of 900  $\text{Wh L}^{-1}$ , LLZO membranes should be even thinner and have higher porosities of 40  $\mu\text{m}$  and 40%, respectively. Notably, as shown in Fig. 2c, the use of porous LLZO membranes with a 10  $\mu\text{m}$  thin LLZO layer, which acts as an additional protective layer to reduce the probability of the short circuit, the overall porosity and the thickness of the porous part of LLZO membranes should be even higher and thinner, accordingly.

Considering these factors, the FIM group has developed porous LLZO membranes with minimal thicknesses of *ca.* 35  $\mu\text{m}$  and a porosity of around 50%.<sup>[28]</sup> Importantly, these membranes also feature a thin upper dense part, serving as an additional protective layer to mitigate potential short circuits during cell charging. Furthermore, in addition to employing conventional synthesis methods for sintering LLZO, the FIM group is actively engaged in developing a cost-effective fabrication methodology for sintering LLZO membranes. In this pursuit, the group recently devised an ultrafast sintering (UFS) method capable of sintering membranes as fast as within one minute.<sup>[30]</sup> The scheme of the customized ultrafast sintering setup and the microstructure of LLZO membranes before and after UFS are shown in Fig. 3. Among various alternative approaches for low-cost sintering of LLZO, this UFS method stands out as particularly promising. Besides reducing sintering times from hours to seconds, one achieves better control over Li stoichiometry and LLZO microstructure. Moreover, UFS is regarded as a scalable roll-to-roll sintering process, which holds significant potential for streamlining the eventual commercialization of SSBs comprising LLZO electrolytes.

Apart from the work on designing the architecture of LLZO solid-state electrolytes and their fabrication methodology, the poor wettability of LLZO by lithium metal has also been a focus of research for the FIM group. This issue is primarily attributed to the presence of a Li-ion-insulating layer on the LLZO surface, consisting of  $\text{LiOH}$  and  $\text{Li}_2\text{CO}_3$ .<sup>[34]</sup> The existence of this layer be-

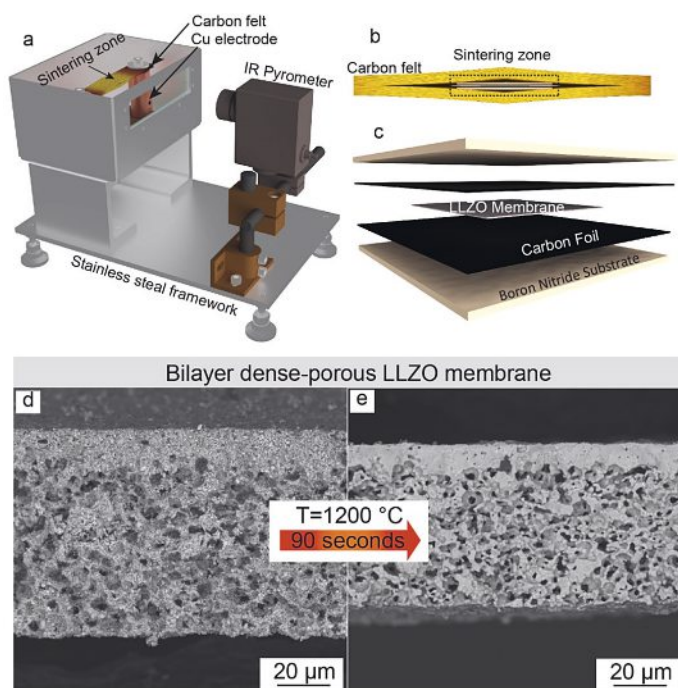


Fig. 3. (a) Schematics of the custom-made ultrafast sintering setup and (b, c) the configuration of the sintering zone. (d, e) Cross-section SEM images of bilayer dense-porous LLZO membranes before (d) and after (e) ultrafast sintering. Reproduced with permission ref. [30]. Copyright 2023, Cell Press.

tween LLZO and Li metal has significant implications for the electrochemical performance of Li-garnet SSBs.<sup>[35–39]</sup> Specifically, it leads to an increase in the interfacial resistance between Li and LLZO, resulting in high-voltage polarization during Li plating/stripping. Moreover, it may contribute to the formation of Li dendrites due to the uneven distribution of applied current density. To address the challenge of poor LLZO wettability by lithium metal, the FIM group has conducted extensive investigations into the use of Sb as an interlayer between LLZO and Li.<sup>[40]</sup> It has been found that Sb can reduce the interfacial resistance between Li and LLZO and enhance the efficiency of Li plating/stripping at the interface. The key factor enabling efficient Li plating/stripping on the Sb-coated LLZO surface is the formation of a Li-Sb alloy, which facilitates effective Li-ion and electronic conduction at the Li/LLZO interface while effectively preventing the formation of voids and Li whiskers during Li plating/stripping.

In concluding this brief overview of the work conducted in the FIM group on SSBs, we note that the current objective is to develop a dual solid-state electrolyte battery concept, incorporating a reductively stable LLZO electrolyte on the Li anode side and a highly Li-ion conductive argyrodites-type  $\text{Li}_6\text{PS}_5\text{X}$  ( $\text{X} = \text{Cl}, \text{Br}, \text{I}$ ) sulfide-based electrolyte on the cathode side. This innovative solid-state concept, combining LLZO and sulfide-based electrolytes, holds the potential to maximize both the high energy and power density of SSBs.

## 2.2 The Research Activities in the Laboratory Materials for Energy Conversion (Empa/ETHZ/EPFL)

SSBs with lithium metal and sodium metal anodes have been investigated in the laboratory Materials for Energy Conversion (MEC, Corsin Battaglia) since its inception in 2014. In an earlier study, the lab compared lithium and sodium metal dendrite formation at the Li/LLZO and Na/Na- $\beta''$ -alumina interface.<sup>[41]</sup> Na- $\beta''$ -alumina is an archetypical solid ion conductor, already deployed in commercial high-temperature sodium-nickel-chloride and sodium-sulfur batteries, with high chemical stability in contact with

sodium metal and an ion conductivity exceeding  $1 \text{ mS cm}^{-1}$  at room temperature.

A practically negligible interfacial resistance  $< 10 \text{ Ohm cm}^2$  was achieved at the Li/LLZO and Na/Na- $\beta''$ -alumina interface by heating LLZO and Na- $\beta''$ -alumina to  $900 \text{ }^\circ\text{C}$  in argon and bringing them into contact with lithium and sodium metal, respectively, after cool down.<sup>[41,42]</sup> Interestingly, stripping plating experiments in symmetric Li/LLZO/Li and Na/Na- $\beta''$ -alumina/Na cells showed that the current density at which dendrites form is roughly a factor of 10 higher for the Na/Na- $\beta''$ -alumina/Na cells than for the Li/LLZO/Li cells as shown in the Arrhenius plot in Fig. 4a, qualifying Na/Na- $\beta''$ -alumina for fast charging applications. The same data is shown in Fig. 4b as a function of the homologous temperature, *i.e.* normalized by the melting temperature of the lithium and sodium metal, respectively. As can be seen from Fig. 4b, the data points for Li/LLZO/Li cells and Na/Na- $\beta''$ -alumina/Na cells align in this representation, indicating that the higher resilience to dendrite formation is rather a property of the alkali metal than of the electrolyte. In fact, the lower melting temperature of sodium metal compared to lithium metal results in higher sodium self-diffusion, which proves effective in pushing the onset current density for void formation at the interface during stripping and consequently also for dendrite formation during subsequent plating to higher values. Voids and a dendrite can be observed in the cross section in Fig. 4c.

The properties of ceramic electrolytes also strongly depend on their phase content and microstructure, which are highly sensitive to processing conditions.<sup>[43–48]</sup> Besides the sintering conditions, the correct choice of the solvent employed for *e.g.* cleaning of the sintered ceramics turns out to be crucial to prevent dendrite formation. LLZO and Na- $\beta''$ -alumina are both prone to protonation in classical solvents including alcohols and acetone, resulting in the replacement of lithium and sodium by protons. The combination of electrochemical impedance spectroscopy, X-ray diffraction, and X-ray photoelectron spectroscopy revealed that (partially) protonated LLZO, designated as HLLZO, exhibits a much lower thermal stability than LLZO, leading to the formation of secondary  $\text{La}_2\text{ZrO}_7$  and  $\text{ZrO}_2$  phases at temperatures as low as  $500 \text{ }^\circ\text{C}$ .<sup>[43]</sup> Protonation of LLZO can be avoided by refraining from using protic and acidic solvents and using high  $\text{pK}_a$  solvents such as hexane instead, resulting in much more stable lithium metal stripping and plating. Furthermore, as an elegant alternative to traditional ceramic processing with pore formers, the method of fabricating bilayer porous/dense and trilayer porous/dense/porous LLZO membranes taking advantage of the volume contraction of garnet-type protonated HLLZO during thermal decomposition into  $\text{La}_2\text{ZrO}_7$  and  $\text{ZrO}_2$  was patented by the MEC lab.<sup>[44,49]</sup> The porous LLZO layer can be melt infiltrated with lithium metal as shown in Fig. 4d, thereby increasing the contact area between the electrolyte and the lithium metal and consequently reducing the local current density, providing an effective means to prevent dendrite formation also at higher (global) current densities. However, continuous repeated charging at current densities of  $\sim 10\text{--}12 \text{ mA cm}^{-2}$ , corresponding to charging rates of 2–3 C with high-capacity cathodes with  $4\text{--}5 \text{ mAh cm}^{-2}$ , remains a challenge. Operated above their melting temperature, alkali metal anodes were demonstrated to repeatedly charge and discharge with a cumulative capacity  $> 10 \text{ Ah cm}^{-2}$ , corresponding to 2000 cycles with  $5 \text{ mAh cm}^{-2}$  electrodes, at  $1000 \text{ mA cm}^{-2}$  or 200 C without dendrite formation, thanks to much increased self-diffusion preventing void formation at the interface to the electrolyte.

While Li/LLZO and Na/Na- $\beta''$ -alumina anode/membranes were integrated successfully in different proof-of-concept dual-solid-electrolyte SSB lab cells,<sup>[44,50]</sup> the assembly of larger cells remains a significant challenge due to the fragility of the ceramic membranes. Na- $\beta''$ -alumina membranes with a surface area of  $\sim 100 \text{ cm}^2$  were fabricated and integrated successfully in

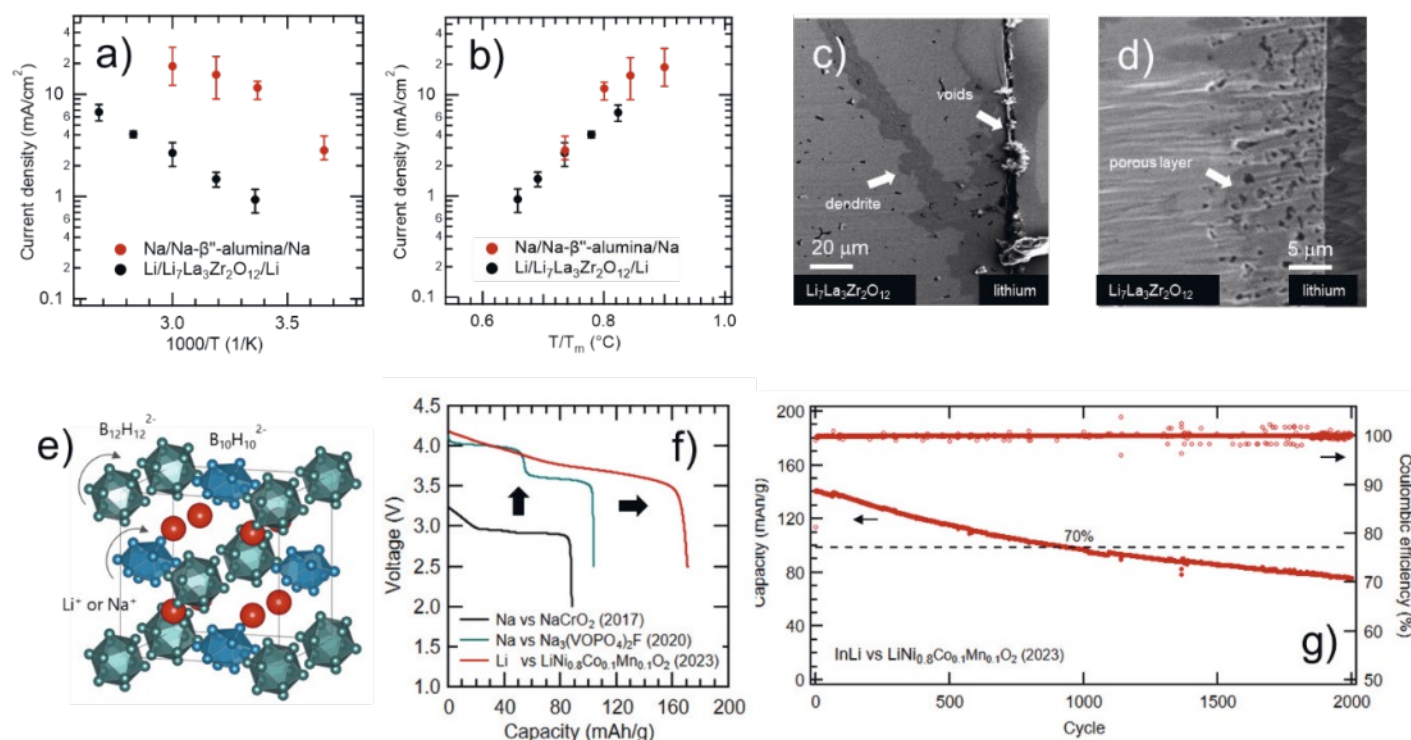


Fig. 4. (a) Arrhenius plot of the current density at which dendrite formation shorts the Li/LZZO/Li and Na/Na- $\beta'$ -alumina/Na symmetric cells,<sup>[41]</sup> (b) same data as in (a) but plotted as a function of the homologous temperature normalized by the melting temperature of the alkali metal, (c) scanning electron microscopy image of the cross section across a LZZO/Li interface with voids at the interface and a lithium metal dendrite propagating away from the interface into the bulk, (d) LZZO/Li interface with porous LZZO layer melt infiltrated by Li metal, (e) atomic structure of fcc *closo*-hydroborate anion lattice consisting of  $B_{12}H_{12}^{2-}$  and  $B_{10}H_{10}^{2-}$  anions (H atoms are not shown) and the mobile  $Li^+/Na^+$  occupying interstitial sites, (f) evolution of the discharge voltage-capacity characteristics for hydroborate-based SSB, the area under the curves represent the discharge energy density, (g) evolution of the cell capacity during long-term cycling.<sup>[57,58,60]</sup>

sodium-nickel-chloride batteries operated at 300 °C,<sup>[51]</sup> but the thickness in the order of 1 mm needs to be reduced to a few 10s of  $\mu\text{m}$  to allow operation at room temperature and to achieve the energy density targets. The brittleness of ceramic electrolytes makes it also difficult to integrate them with the cathode, because the cathode particles typically undergo a volume change during dis-/charging resulting in electrolyte cracking.

For these reasons, the MEC lab has also a strong focus on developing solid electrolytes that are ductile, can be compacted without sintering, while offering high ion conductivity at room temperature and compatibility with alkali metal anodes and high-voltage cathodes. A promising, yet underexplored, class of materials that fulfils many of these requirements are the hydroborates.<sup>[15]</sup> Hydroborates are salts with complex anions. Rapid advances were made with lithium and sodium hydroborates, in particular with the *closo*-hydroborate and *closo*-hydrocarbaborate anions, which exhibit high electrochemical stability in contact with alkali metal anodes and the highest oxidative stability. Key to high cation conductivity is the stabilization of a high symmetry periodic anion lattice at room temperature typically accomplished by mixing at least two different anions as shown in Fig. 4e.<sup>[52–55]</sup> *Closo*-hydroborate anions carry two negative charges, while *closo*-hydrocarbaborates carry one negative charge, allowing for a large variety of crystal structures with different cation fillings. The interested reader is referred to two recent reviews on the topic by our lab.<sup>[15,56]</sup>

Efforts to integrate hydroborate electrolytes into SSBs have culminated in the demonstration of a sodium SSB with a state-of-the-art 4 V-class  $\text{Na}_3(\text{VOPO}_4)_2\text{F}$  cathode<sup>[57–59]</sup> and more recently a lithium SSB with a state-of-the-art 4 V-class  $\text{LiNi}_{0.8}\text{Co}_{0.1}\text{Mn}_{0.1}\text{O}_2$  cathode,<sup>[60]</sup> both featuring a capacity retention >70% after 1000 dis-/charge cycles as shown in Fig. 4f and 4g. Due to the risk of dendrite formation, cycling at room temperature remains limited

to relatively low current densities. Another major challenge is the currently high cost of *closo*-hydroborates and *closo*-hydrocarbaborates. While a low-temperature *solvo*-thermal synthesis route for *closo*-hydroborates has been proposed by our lab in collaboration with the group of Prof. Hans Hagemann (retired), Université de Genève,<sup>[61]</sup> the availability of hydroborates is still restricted to relatively small quantities, not yet allowing trials on industrial pilot battery cell manufacturing lines. The MEC lab is actively working towards building a consortium to solve this issue, encouraging also the involvement of Swiss Chemical Society members and the Swiss chemical industry.

In parallel to the developments on hydroborate electrolytes, MEC group has also investigated a number of different polymer electrolytes. While polyethylene oxide-based electrolytes show good compatibility with lithium metal anodes, their conductivity at room temperature  $< 0.01 \text{ mS cm}^{-1}$  is not sufficient to enable battery operation at room temperature and the oxidative stability is limited to low-voltage cathodes such as  $\text{LiFePO}_4$ .<sup>[62]</sup> Polysiloxane-based electrolytes were also explored, but with similar conclusions.<sup>[63]</sup> More recently, the focus shifted to polymerized-ionic-liquid-based electrolyte in particular  $\text{Pyr}_{13}$ -FSI-derived polymers, in which the cation is polymerized.<sup>[64]</sup> The polymerized cation chains have the advantage of reducing lithium-ion coordination with the polymer, which is a major issue in PEO-based electrolytes, promoting high cation mobility and ion conductivities in the order of  $1 \text{ mS cm}^{-1}$  at room temperature. While the FSI anion is not stable in contact with lithium metal, FSI is known for forming a passivating interface layer with relatively high lithium-ion conductivity. The  $\text{Pyr}_{13}$ -FSI-derived polymer excels in terms of oxidative stability, enabling the integration with 4 V-class  $\text{LiNi}_{0.8}\text{Co}_{0.1}\text{Mn}_{0.1}\text{O}_2$  and even a 5 V-class  $\text{LiMn}_{1.5}\text{Ni}_{0.5}\text{O}_4$  cathode, demonstrating stable cycling over several hundred dis-/charge cycles. Projections from industrial partner Solvionic show that

this kind of polymer electrolyte will be available at a price of less than 80 \$ kg<sup>-1</sup> when benefitting from the economy of scale when scaling production to 50 t per year. The availability, relatively low cost, and excellent performance of the polymerized-ionic-liquid-based electrolytes make them a strong contender for a competitive solid-state battery technology capable of reaching the 1200 Wh L<sup>-1</sup> and 450 Wh kg<sup>-1</sup> targets for SSB, when implemented into optimized cells.

### 2.3 The Research Activities in the Battery Materials and Diagnostics Group (BMD, PSI)

Alongside promising SSB configurations based on oxide ceramic and polymer SSEs, sulfide glass-ceramic SSEs offer alternative material systems already widely established by many research teams and industry.<sup>[13,65]</sup> Their main advantages result from their low density, competitive ionic conductivity at room temperature beyond 10<sup>-2</sup> S cm<sup>-1</sup>, low resistance at the grain boundaries, and especially their ease of synthesis and processing at room temperature for a reduced separator thickness (≤ 30 μm) and a subsequent increase in the cell energy density.<sup>[66,67]</sup> However, sulfide SSEs still suffer from multiple limitations, among them the severe interfacial (electro-) chemical and mechanical instabilities with the anode and cathode materials, which has a direct impact on the Li-ion transport leading to an interface impedance rise limiting drastically the cell cycling performance. As an example, a wide-spread solid electrolyte is β-Li<sub>3</sub>PS<sub>4</sub> (βLPS), which undergoes reduction below 1.7 V vs Li<sup>+</sup>/Li and oxidation above 2.3 V vs Li<sup>+</sup>/Li.<sup>[68,69]</sup> Additionally, the large volume changes of the anode active (AAM) and the cathode active material (CAM) lead to cracks, voids formation and contact loss between the different cell components.<sup>[3]</sup> Finally, enabling thin metallic lithium or Li reservoir-free anodes requires also tremendous efforts to prevent dendrites, ‘dead Li’ and void formation at the interface with the SSE.<sup>[70]</sup>

The current research efforts in the Battery Materials and Diagnostics Group (BMD, Mario El Kazzi) aims to shed light on the fundamental understanding of the interface chemo-mechanical processes of sulfide-based SSEs and to mitigate interface resistivity alongside improved battery life cycle performance. Different configurations are explored by the BMD group as shown in Fig. 5 with the goal to push the limits of achievable energy densities towards 500 Wh kg<sup>-1</sup> and beyond, based on different types of anode materials. A range of thiophosphate SSEs combined with so-called high voltage cathode materials (e.g. nickel-rich, cobalt

low LiNi<sub>x</sub>Co<sub>y</sub>Mn<sub>z</sub>O<sub>2</sub>) is employed as cathode composites, together with different anode types (e.g. Si/graphite, thin metallic lithium or Li reservoir-free). BMD group is committed to address those challenges by the development of advanced *in situ* and *operando* surface and bulk characterization methods using laboratory and synchrotron facility techniques at the Swiss Light Source (SLS). Therefore, we designed custom-made: (i) electrochemical cells for accurate and reliable electrochemistry cycling of pellet-type SSB materials; (ii) *operando* electrochemical cells for the various analytical methods and adapt/develop the synchrotron beamline end-stations to the requirements for SSB studies. Furthermore, the BMD group dedicates large efforts to the interface engineering, with the purpose of mitigating the interface reactivities and improving cycling stability (Fig. 5). Thin inorganic coatings are applied to directly modify the surface properties of the cathode, SSE and anode materials using various synthetic methods like gas-solid, ultra-high-vacuum thin film deposition and wet/dry chemistry.

At first, we highlight, the development of different generations of custom-made SSB cells which is the first crucial step to accurately evaluate and determine the electrochemical properties and cycling performances of SSBs, including SSE conductivity, specific capacity or long-term capacity retention. The generation 1 (*gen.1*) cell shown in Fig. 6a was developed in 2016 to address the limited commercial options for cycling SSBs at the time.<sup>[71]</sup> These cells allowed to cycle reproducibly pellet-type batteries under high pressure (20 MPa – 400 MPa) and were used to characterize the electrochemical properties of several SSB working electrodes, including graphite-βLPS,<sup>[72]</sup> Li<sub>4</sub>Ti<sub>5</sub>O<sub>12</sub>-LPS<sup>[68]</sup> or LiCoO<sub>2</sub> and LiNi<sub>x</sub>Co<sub>y</sub>Mn<sub>z</sub> (NCM).<sup>[73–75]</sup> However, the *gen.1* cell exhibits two main drawbacks, as it relies on external pressure for tightness and the lowest achievable pressure below 20 MPa poses a limit in the study of metallic lithium anodes. Finally, the industry requirement for SSE to operate below 5 MPa could not be fulfilled by the *gen.1* cell, inhibiting application of relevant studies.

In response to such limitations, we have developed the next generation 2 (*gen.2*) cell (see Fig. 6a), capable of functioning at very low stabilized pressures (80 MPa – 2 MPa) thanks to the single axial screw and the incorporation of a disk spring that ensures the maintenance of constant pressure during the long cycling process. Additionally, with the improved O-ring compression system exceptional tightness of 10<sup>-8</sup> mbar·l s<sup>-1</sup> can be achieved. The *gen.2* cell has been used successfully in metallic lithium applications

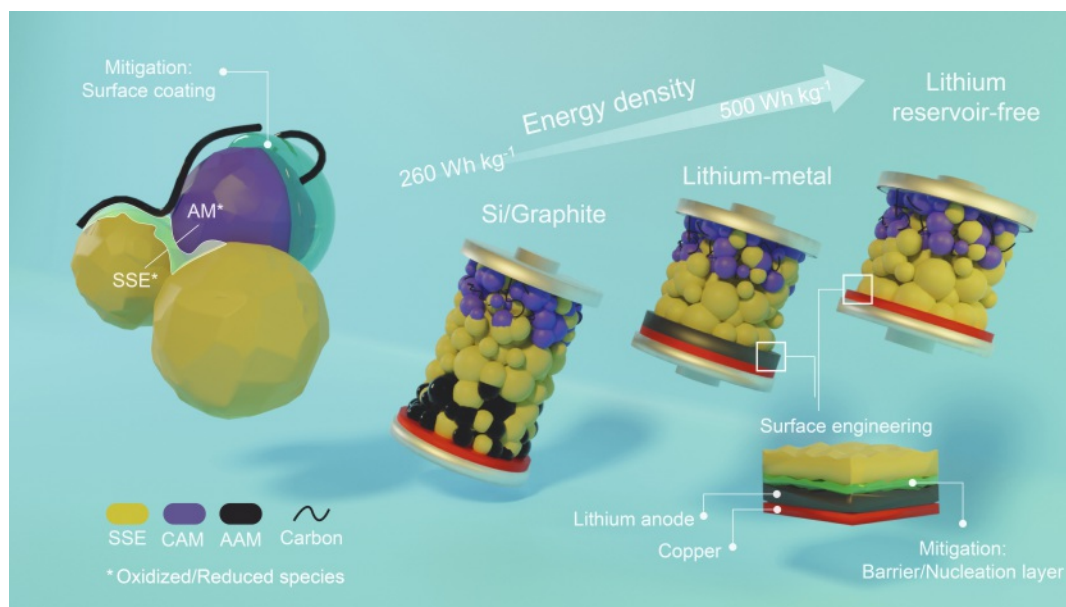


Fig. 5. BMD group addresses different types of sulfide SSE-based SSB combined with high voltage CAM (e.g. LiNi<sub>x</sub>Co<sub>y</sub>Mn<sub>z</sub>O<sub>2</sub>) and various configurations of AAM (e.g. Si/graphite anode thin lithium metal and lithium reservoir-free), with the aim to achieve higher energy densities beyond 500 Wh kg<sup>-1</sup>. We highlight different interface degradation mechanisms together with BMD's approach to mitigate them in a targeted surface engineering.

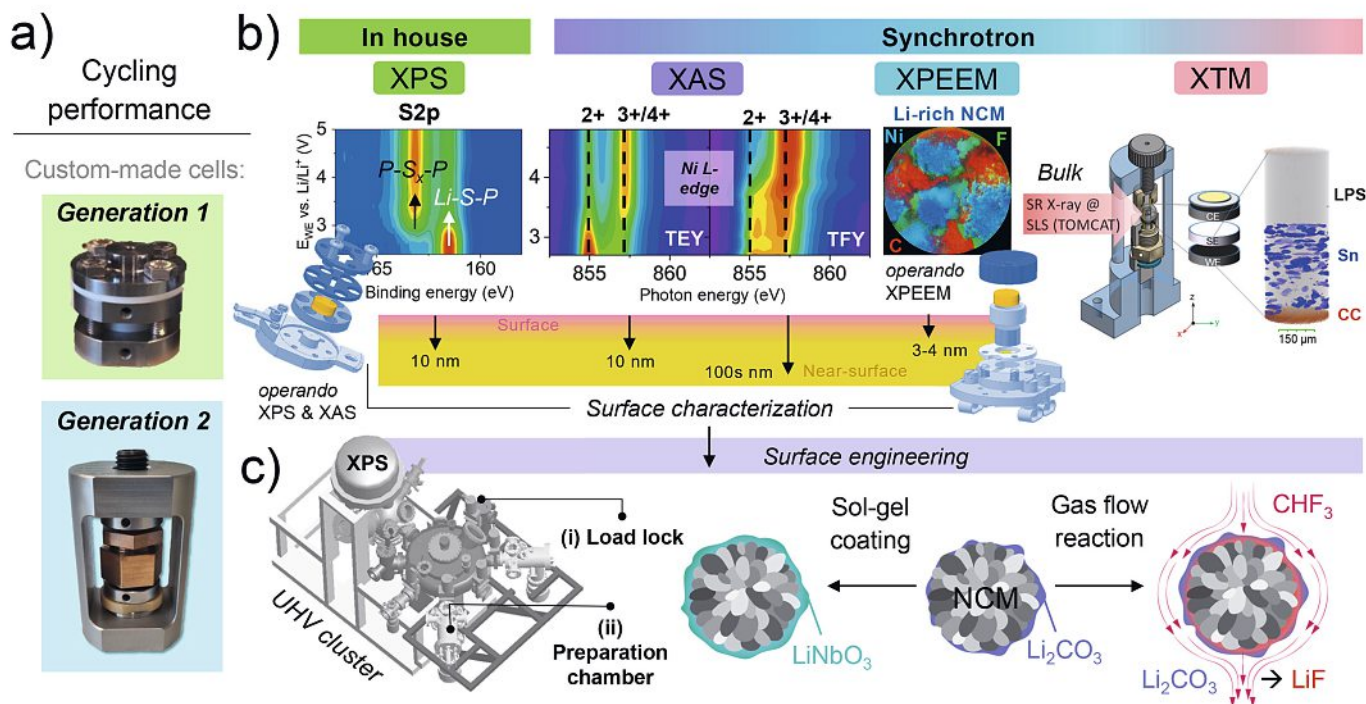


Fig. 6. Overview of the SSB research activities in the BMD group at PSI, including (a) different standardized cells for cycling performance evaluation of new battery materials and systems, (b) in-house and synchrotron X-ray characterization from surface to bulk, as well as (c) surface engineering capabilities from PVD thin film coating to sol-gel and gas-solid coating methods.

to enable electrochemical characterization outside the glovebox setups.

Next, we highlight the creation and development of a unique complementary *in situ/operando* non-destructive surface characterization platform (Fig. 6b) combining in-house X-ray photoelectron spectroscopy (XPS) and X-ray synchrotron techniques located at the SLS, employing X-ray absorption spectroscopy (XAS), X-ray photoemission electron microscopy (XPEEM) and X-ray tomographic microscopy (XTM). This state-of-the-art platform allows the study of the surface, near surface and interface to understand the (electro-) chemical reactivity, charge carrier mobility as well as chemo-mechanical limitations between the SSE and different active materials (AMs).<sup>[76]</sup> Such interfaces are commonly buried, difficult to access and conventional characterization methods fail to perform their analysis non-destructively, especially during battery operation. BMD has addressed the necessity of developing such advanced characterization at multiple scales of depth probing for both post-mortem and *in situ/operando* studies. As an example, conventional laboratory XPS with high surface-sensitivity ( $\sim 10$  nm) is a powerful technique to study the chemical and electronic properties of materials. It is known to resolve the individual redox-by-products of the SSEs and *operando* studies of the BMD group could correlate accurately the redox processes in SSBs with their voltage dependency.<sup>[69,77]</sup> In addition, *operando* XAS<sup>[78]</sup> with its higher sensitivity towards transition metals (TMs) allows for a depth-profiling by following simultaneously signals evolving in real-time on the surface ( $\sim 10$  nm) and near-surface ( $\sim 100$  nm) of a composite working electrode (see Fig. 6b), using total electron yield (TEY) and total fluorescence yield (TFY) detection modes, respectively. Furthermore, *operando* XPEEM<sup>[79]</sup> is employed as a highly surface sensitive analytical technique capable of providing a unique combination of the nanoscale lateral resolution ( $\sim 50$  nm) and the spectroscopic capability of XAS, confined within a depth analysis range of 3–4 nm. A great advantage of synchrotron light is the tuneable energy which allows for a broad range of elemental detection, including tender X-rays to detect TMs, S, P and Cl K-edges, as

well as O, C K-edges and TMs, S, P and Cl L-edges with soft X-rays. Besides the utilization of synchrotron light for chemical surface and interface-oriented studies, the internal volume change and crack formation of the SSBs is very difficult to assess by *ex situ* experiments. Therefore, the application of *operando* XTM allows for a time-resolved 3D imaging of the SSB interior during operation with sub- $\mu\text{m}$  resolution.<sup>[80]</sup> The successful utilization of this technique revealed the anisotropic volume expansion of AMs, the mechanism of crack formation and propagation in the SSE as well as the impact of mechanical deformation on the tortuosity evolution and the Li-ion transport (Fig. 6b). Further, the reliability of such elaborate *operando* analysis is the result of very compatible, close to standard cell application, custom-made *operando* cells, with the 3 different models shown in Fig. 6b for XPS/XAS, XPEEM and XTM.

Utilizing the advantage of such powerful surface analysis, we can drive the mitigation of interface phenomena towards higher (electro-) chemical stability with a targeted surface engineering (see Fig. 6c) for various SSEs, CAMs, AAMs and additives. For example, BMD group is equipped with an ultra-high vacuum (UHV) cluster with a base pressure  $\sim 10^{-9}$  mbar connected to the XPS spectrometer, employing Ar sputtering for surface treatment and depth profile analysis, RF sputtering for thin film deposition, electron gun evaporator for various metals or oxides thin film depositions, and different gas entry. Such a unique setup offers a great variety of surface modifications (*e.g.* Li metal, current collector foils or pelletized SSEs), with a direct *in situ* XPS chemical analysis under vacuum. For thin coatings of powders with micron to nanosized particles, wet-chemical methods (*e.g.* sol-gel) or gas-solid reactions with reactive gasses are more eligible. On one hand, thin coatings of the CAM can be fabricated by using sol-gel methods with *e.g.*  $\text{LiNbO}_3$  being the most represented choice in literature.<sup>[81]</sup> On the other hand, thin ( $\sim 1$ – $2$  nm) uniform LiF surface coatings were successfully performed on high voltage cathode and SSE materials using a custom-made gas flow-type reactor with a mild fluorinating agent (*e.g.*  $\text{CHF}_3$ ). The thin LiF layer significantly improved the interface stability between the

cathode materials and the electrolyte at high operating voltage above 4.3 V vs Li<sup>+</sup>/Li.<sup>[82]</sup> This method is facile, effective, scalable and environmentally friendly to consume a stock of CHF<sub>3</sub>, a potent greenhouse gas.

In conclusion, we highlight the unprecedented advantage of combining *operando* XPS, XAS and XPEEM to non-destructively probe the degradation mechanisms taking place at the electrified interface of SSE/AMs at multiple depth scales. Together with the bulk analysis capabilities of *operando* XTM we generate a comprehensive picture of performance limiting degradation mechanisms in SSBs. Combined with various surface engineering capabilities at PSI, we can drive the nature of detrimental interface phenomena towards a more beneficial surface chemistry and structure for high energy density SSBs. An approach that is eminently suitable for the study and navigation of battery failure more generally.

#### 2.4 The Research Activities in the Group of Thin Films and Photovoltaics (Empa)

Thin film batteries (TFBs) are solid-state batteries in which each component of the battery is at most a few micrometers thick, and they are stacked on top of each other in a layered fashion.<sup>[83]</sup> TFBs are typically made using vacuum techniques to deposit a wide range of materials in the form of dense and homogeneous layers with precise control of their thickness. Due to the short diffusion pathways given by the thin layers, thin-film batteries can be cycled at high C-rates.<sup>[84,85]</sup> In addition, they have shown stable cycling performance of over 10,000 cycles with a capacity loss of less than 10%.<sup>[86]</sup> However, their broad applicability is limited by their low areal capacities (<0.1 mAh cm<sup>-2</sup>). TFBs can also be used as model systems thanks to their well-defined, layered architecture to test the combinations of materials as well as to characterize interfaces and fundamental phenomena without the interference

of conductive additives, porosity *etc.* In the Laboratory for Thin Films and Photovoltaics at Empa we use the TFBs as model systems to study novel materials and their combinations, such as materials for electrodes and solid-state electrolytes, coatings for better interfaces as well as device manufacturing approaches and device architectures – stacked TFBs, TFBs on flexible substrates *etc.* (see Fig. 7). In our Laboratory we employ a wide scope of characterization methods to study the TFBs ranging from more traditional material science tools such as X-ray diffraction, electron and light microscopy, through electrochemical methods: galvanostatic cycling, cyclic voltammetry, electrochemical impedance spectroscopy, galvanostatic intermittent titration technique, transient current measurements to advanced characterization such as time-of-flight secondary ion mass spectroscopy, X-ray photoelectron spectroscopy, cryo-airless electron microscopy and others.

As magnetron sputtering is one of the main focus points of our Laboratory, we have developed a scalable co-sputtering approach for depositing high-quality oxide solid-state electrolyte thin films, such as LLZO and LiPON.<sup>[92]</sup> In this way, we have produced crystalline LLZO thin films exhibiting record ionic conductivities of  $1.9 \times 10^{-4}$  S cm<sup>-1</sup> by co-sputtering LLZO and Li<sub>2</sub>O.<sup>[92]</sup> High ionic conductivities with the low thickness, led to a significantly reduced electrolyte's area-specific resistance.<sup>[92]</sup> Furthermore, we investigated the interface of LCO and LLZO and introduced two types of interlayers to improve its characteristics: (1) an *in situ* lithiated Nb<sub>2</sub>O<sub>5</sub> diffusion barrier layer that effectively reduces the charge-transfer impedance of the LLZO-LCO interface and enables higher current rates compared to a non-modified LLZO-LCO interface,<sup>[89,93]</sup> and (2) a thin-film LLZO layer without annealing (amorphous), which has a similar effect to the lithiated Nb<sub>2</sub>O<sub>5</sub> allowing for lowered interfacial resistance, which in turn lowered

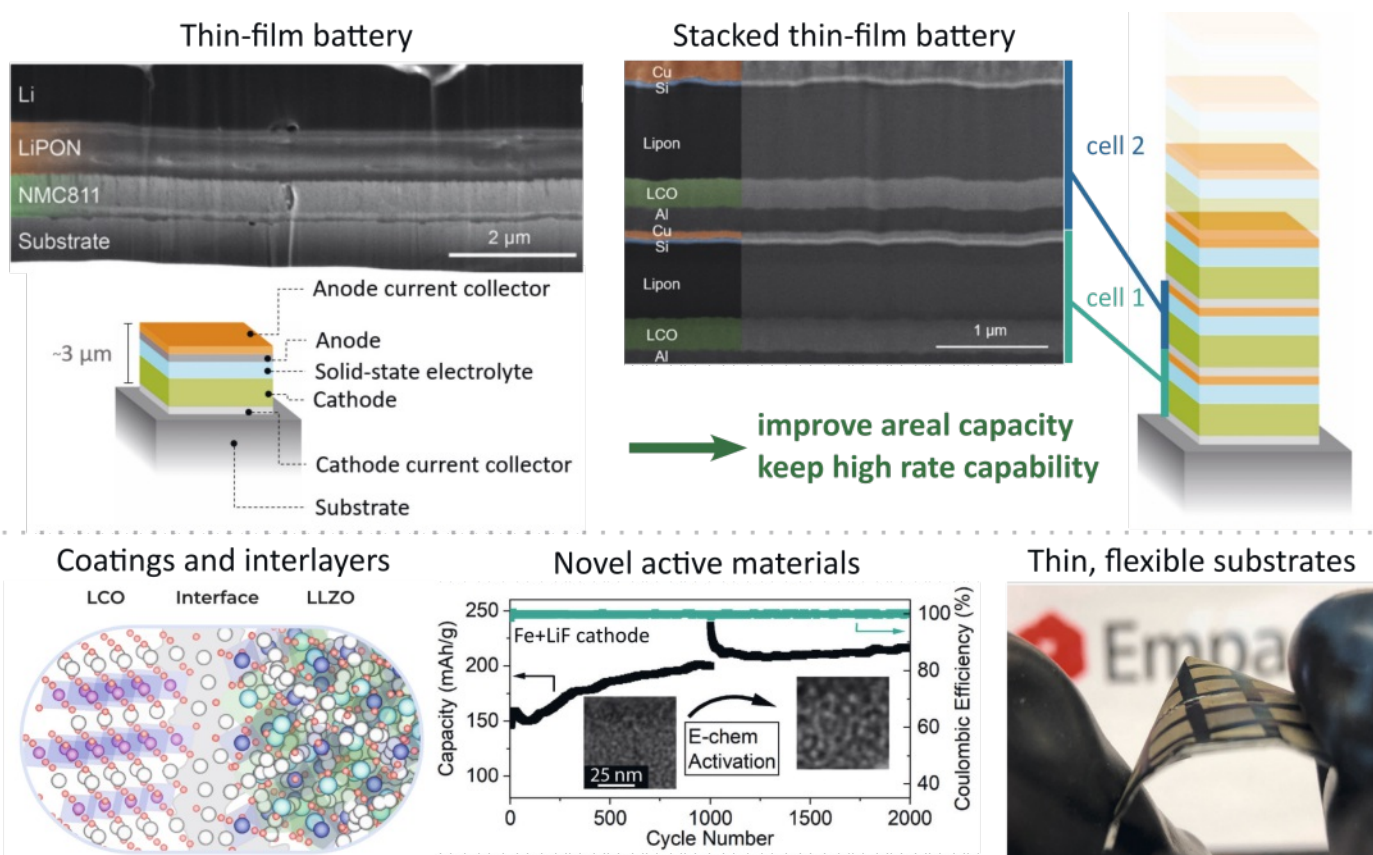


Fig. 7. Top panel: schematic of a thin film battery and a monolithically stacked thin film battery. Adapted with permission from refs. [87] and [88]. Bottom panel: examples of areas of interest of the Laboratory for Thin Films and Photovoltaics. Adapted with permission from refs. [89–91] and adapted under CC-BY 4.0 license ref. [90]. Note that further permissions related to the material excerpted should be directed to the original publisher.



the overpotentials for Li plating and higher critical current densities (currents at which the cells would fail).<sup>[94]</sup>

We also benchmarked interlayers on the anode side – seed layers between the anode current collector and the solid-state electrolyte for improved Li plating and stripping behaviour. Reversible Li stripping and plating at high current densities is crucial for the performance of all Li-metal and ‘anode free’ (without Li reservoir) batteries. Using TFBs as a model system, seed layers of Pt, Au and amorphous carbon deposited using magnetron sputtering at the interface between the solid electrolyte and the anode current collector were studied. All seed layers improved the kinetics of Li plating/stripping, reduced the overpotentials and enabled higher critical current densities of over 8 mA cm<sup>-2</sup>. While Pt and Au alloy with lithium, the amorphous carbon interlayers remained intact during stripping and plating, resulting in homogeneous lithium metal plating and stripping at room temperature without applied external pressure.<sup>[95,96]</sup>

Another area of battery research that can benefit from the model system aspect of TFBs are novel electrode materials. We reported the first thin-film solid state LiNi<sub>0.8</sub>Mn<sub>0.1</sub>Co<sub>0.1</sub>O<sub>2</sub> NMC811 battery with a LiPON electrolyte that showed excellent cycling stability over 1000 cycles at 4 C. Moreover, this cycling stability was achieved with the voltage range extended to 1.5 V (from a normal lower cut-off voltage of 3 V). In this way, the NMC811 cathode can be over lithiated and store additional lithium in each cycle. Therefore, the reversible capacity in the first 50 cycles was increased to about 250 mAh g<sup>-1</sup>, which is a significant improvement over conventional NMC811.<sup>[87]</sup> Within the cathode materials, we are also actively exploring the landscape of conversion cathodes. We demonstrated that Fe and LiF based conversion cathode can be used with LiPON solid electrolyte and Li metal anodes. In these cells, the Fe-LiF cathodes undergo a process of nanoscale restructuring during cycling that is C-rate dependent. By choosing the right current density (approx. 6 C), this electrochemical activation allowed for 2000 reversible cycles without capacity fade. On the contrary, the capacity of the cells increased over the cycling protocol to 480 mAh g<sup>-1</sup> cathode, which is very close to the theoretical capacity of this system (498 mAh g<sup>-1</sup>). This highlights how a thin-film, pure materials system can be utilized to study fundamental properties of said materials.<sup>[90]</sup>

We also investigate novel crystallization methods. In particular, rapid photonic annealing, or flash lamp annealing, can be used to crystallize thin-film cathodes without exposing other parts of the battery to high temperatures enabling crystalline active materials (which tend to make higher performance cathodes) on heat-sensitive substrates, potentially allowing for the use of flexible substrates, while also increasing the speed of crystallization from hours to minutes.<sup>[91]</sup>

Finally, to address the low areal capacity of TFBs compared to other battery types, we explore the potential of stacking multiple TFBs monolithically on top of each other, thus improving the areal capacity without compromising the dense, homogeneous layered structure and short diffusion pathways that facilitate high C-rate operation. We have demonstrated a working stack of two TFBs,<sup>[88]</sup> proving the feasibility of this approach while highlighting all the necessary development steps needed to bring stacked TFBs to their full potential. A thermo-electric model showed that stacked thin-film batteries can achieve a specific power of tens of kW per kg, which is ten times higher than what is possible with the current Li-ion batteries.<sup>[88]</sup>

## 2.5 The Research Activities in the Group of Process Optimization in Manufacturing (Berner Fachhochschule)

While SSBs with lithium metal anodes offer opportunities for improved and simplified cell manufacturing, they also present new challenges. For example, polymer-based solid electrolytes can be co-processed with cathode materials to form a so-called

catholyte.<sup>[97]</sup> The formation of catholyte layers can be achieved with scalable roll-to-roll technologies such as slot die coating or dry extrusion. Prefabrication of these catholyte layers has implications for upstream cell manufacturing processes that need to be addressed to achieve an optimal manufacturing process. The use of lithium metal anodes presents a number of challenges for large-scale manufacturing. Forming thin film lithium metal anodes using a mechanical calendaring process is difficult and costly. In addition, lithium metal is very sticky to many surfaces and reacts easily with many materials. As a result, the machine and process design options for cutting and stacking lithium metal anodes into a cell are very limited.

The Process Optimization in Manufacturing research group at the Bern University of Applied Sciences is investigating novel methods and processes for the production of both LIBs and SSBs. One proposed strategy to mitigate dendrite growth in lithium metal cells is the use of thermotropic ionic liquid crystals (TILCs). When heated the TILC undergoes a phase change that can mechanically break dendrites and refresh the interphase between the electrolyte and lithium metal.<sup>[98]</sup> In this context and within the framework of the H2020 project HIDDEN,<sup>[99]</sup> we have investigated an alternating current-based heating approach for pouch cells to induce the phase change of the TILC. Furthermore, we have established a lab-scale process for lithium metal-based pouch cells. The line allows flexible cell configurations in the Ah range. Cells originating from this line have been used in these studies.<sup>[100,101]</sup> To address the processing challenges with lithium metal anodes we have developed an optimized laser cutting process to shape the electrodes. An uneven lithium metal surface strongly promotes the formation of dendrites and thus accelerates cell aging. The cutting process of lithium metal anodes must therefore leave as few traces on the electrode surface as possible. Fig. 8 shows the difference in melt formation at the cut edge of a non-optimized laser cutting process compared to our optimized process. We have demonstrated that our laser process can meet the desired requirements using typical laser equipment of today’s LIB production.

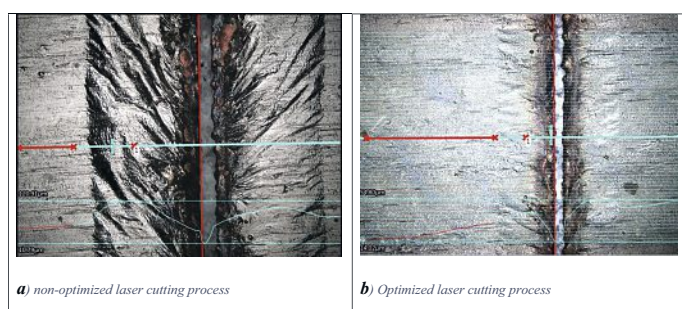


Fig. 8. Digital microscope top-view images of the cut edge of laser processed lithium metal electrodes.

LIB production in general and SSB in particular suffer from a lack of dedicated in-line measurements to assess the quality of intermediate products and to effectively control the processes. This hinders the transition from statistical process control to advanced process control. To help to overcome these problems, we have developed a device for spatially resolved resistance measurements of electrodes. The device can detect defects in electrodes or solid-electrolyte-cathode composites that may not be optically visible, such as poor adhesion of the active material to the substrate, or short circuits when the electrolyte has also a separation functionality, as is common in SSBs. Within framework of the Horizon Europe project SOLiD,<sup>[102]</sup> we have ongoing activities to develop new measurement technologies and use them together with existing ones for closed-loop control and optimization of cathode

composite (active material and solid electrolyte) manufacturing. The developments will be demonstrated on a relevant scale for the slot die coating of a polymer-based solid separator electrolyte.

### 3. Conclusions and Outlook

The field of SSBs has undoubtedly made significant progress in the last decade, driven by extensive research efforts focused on the material optimization and new advances in *in situ/operando* characterization methods. Swiss research institutions have been at the forefront of these innovations, as highlighted in this paper. Nevertheless, SSB as of today is an immature technology to enter the large battery market and it still requires further advancements on multiple fronts, as briefly outlined below.

On the anode side, enabling thin lithium metal ( $\leq 5 \mu\text{m}$ ) is crucial to boost the energy density. Ultimately, moving to the Li-reservoir free anode is desired which not only increases the energy density further but also offers facile and low-cost cell manufacturing due to lower safety requirements in the absence of metallic Li during cell assembly. However, considering the issues stemming from the large volume changes of Li during plating/stripping, as well as its poor chemical compatibility with most classes of SSEs and poor wettability with the current collector, future research efforts will be oriented towards the interface chemical engineering. This is realized through nucleation and barrier layers on top of the thin lithium or current collector, introducing the 3D current collector, 3D lithium or the use of bilayer dense/porous solid electrolyte membranes (e.g. LLZO).

On the cathode side, despite remarkable progress in improving the electrochemical performance at high operating voltages, the intimate contact between the SSE and the cathode active materials is still considered a major challenge to overcome for both oxides (e.g. LLZO) and sulfide glass-ceramic SSEs. This scepticism stems from several inherent hurdles, primarily the inability of the SSE to accommodate the volume fluctuations of the cathode active materials during operation. As a result, the contact between the active materials, the SSE, and the conductive additives is not maintained, leading to a gradual decrease in the charge storage capacity. In this context, the use of more ductile SSE, such as hydroborate or sulfide SSEs on the cathode side of the SSB, in combination with the application of pressure, should be a better option. Nonetheless, the strategy of applying high pressure, as an additional component to enable pressure application would inevitably reduce the energy density significantly. In this context, the use of soft Pyr<sub>13</sub>FSI-derived polymers as SSE, which exhibit a high degree of oxidative stability, seems to have a very high potential, and requires zero or minimal pressure compared to hydroborate or sulfide SSE. It should be noted, however, that a major challenge to the use of hydroborates is their current high cost. While a low-temperature solvothermal synthesis route for *closo*-hydroborates has been proposed, the availability of hydroborates is still limited to relatively small quantities, which does not yet allow trials on industrial pilot battery cell production lines. Further, protective inorganic coatings of the active materials offer good (electro-) chemical stability for prolonged cycle performance and could potentially counteract certain volume changes, improve interfacial contact resistance, and delimit surface degradation mechanisms with an extension of the electrochemical stability window.

Another critical issue with SSBs based on LLZO or *beta*-alumina is their brittleness and low fracture toughness, which may require specific technological solutions for the sintering and handling thin sub-100-micron membranes in large sizes and their layering. In this context, unlike current liquid electrolyte systems, their manufacturability and material costs are unknown, necessitating careful consideration in the context of possible additional costs.

Finally, it should be noted that while SSBs are intrinsically safe during discharge, there are safety concerns during charging. This requires testing possible failure modes due to short circuits,

using SSBs of large size comparable to standard liquid-based Li-ion systems.

### Author Contributions

The manuscript was written through the contributions of all authors. All authors have given approval to the final version of the manuscript.

Received: April 1, 2024

- [1] J. Janek, W. G. Zeier, *Nat. Energy* **2016**, *1*, 16141, <https://doi.org/10.1038/nenergy.2016.141>.
- [2] Q. Wang, Y. Zhou, X. Wang, H. Guo, S. Gong, Z. Yao, F. Wu, J. Wang, S. Ganapathy, X. Bai, B. Li, C. Zhao, J. Janek, M. Wagemaker, *Nat. Commun.* **2024**, *15*, 1050, <https://doi.org/10.1038/s41467-024-45258-3>.
- [3] T. Schmaltz, F. Hartmann, T. Wicke, L. Weymann, C. Neef, J. Janek, *Adv. Energy Mater.* **2023**, *13*, 2301886, <https://doi.org/10.1002/aenm.202301886>.
- [4] D. H. S. Tan, Y.-T. Chen, H. Yang, W. Bao, B. Sreenarayanan, J.-M. Droux, W. Li, B. Lu, S.-Y. Ham, B. Sayahpour, J. Scharf, E. A. Wu, G. Deyscher, H. E. Han, H. J. Hah, H. Jeong, J. B. Lee, Z. Chen, Y. S. Meng, *Science* **2021**, *373*, 1494, <https://doi.org/10.1126/science.abg7217>.
- [5] L. Zhou, A. Assoud, Q. Zhang, X. Wu, L. F. Nazar, *J. Am. Chem. Soc.* **2019**, *141*, 19002, <https://doi.org/10.1021/jacs.9b08357>.
- [6] J. Janek, W. G. Zeier, *Nat. Energy* **2023**, *8*, 230, <https://doi.org/10.1038/s41560-023-01208-9>.
- [7] F. Okur, Y. Sheima, C. Zimmerli, H. Zhang, P. Helbling, A. Fäh, I. Mihail, J. Tschudin, D. M. Opris, M. V. Kovalenko, K. V. Kravchyk, *ChemSusChem* **2024**, *17*, e202301285, <https://doi.org/10.1002/cssc.202301285>.
- [8] P. Albertus, V. Anandan, C. Ban, N. Balsara, I. Belharouk, J. Buettner-Garrett, Z. Chen, C. Daniel, M. Doeff, N. J. Dudney, B. Dunn, S. J. Harris, S. Herle, E. Herbert, S. Kalnaus, J. A. Libera, D. Lu, S. Martin, B. D. McCloskey, M. T. McDowell, Y. S. Meng, J. Nanda, J. Sakamoto, E. C. Self, S. Tepavcevic, E. Wachsman, C. Wang, A. S. Westover, J. Xiao, T. Yersak, *ACS Energy Lett.* **2021**, *6*, 1399, <https://doi.org/10.1021/acseenergylett.1c00445>.
- [9] K. J. Kim, M. Balaish, M. Wadaguchi, L. Kong, J. L. M. Rupp, *Adv. Energy Mater.* **2021**, *11*, 2002689, <https://doi.org/10.1002/aenm.202002689>.
- [10] A. Banerjee, X. Wang, C. Fang, E. A. Wu, Y. S. Meng, *Chem. Rev.* **2020**, *120*, 6878, <https://doi.org/10.1021/acs.chemrev.0c00101?src=getfr>.
- [11] G. Yoon, S. Kim, J.-S. Kim, *Adv. Sci.* **2023**, *10*, 2302263, <https://doi.org/10.1002/advs.202302263>.
- [12] C. Wang, K. Fu, S. P. Kammampata, D. W. McOwen, A. J. Samson, L. Zhang, G. T. Hitz, A. M. Nolan, E. D. Wachsman, Y. Mo, V. Thangadurai, L. Hu, *Chem. Rev.* **2020**, *120*, 4257, <https://doi.org/10.1021/acs.chemrev.9b00427>.
- [13] S. Randau, D. A. Weber, O. Kötz, R. Koerver, P. Braun, A. Weber, E. Ivers-Tiffée, T. Adermann, J. Kulisch, W. G. Zeier, F. H. Richter, J. Janek, *Nat. Energy* **2020**, *5*, 259, <https://doi.org/10.1038/s41560-020-0565-1>.
- [14] T. Krauskopf, F. H. Richter, W. G. Zeier, J. Janek, *Chem. Rev.* **2020**, *120*, 7745, <https://doi.org/10.1021/acs.chemrev.0c00431>.
- [15] L. Duchêne, A. Remhof, H. Hagemann, C. Battaglia, *Energy Storage Mater.* **2020**, *25*, 782, <https://doi.org/10.1016/j.ensm.2019.08.032>.
- [16] K. V. Kravchyk, D. T. Karabay, M. V. Kovalenko, *Sci. Rep.* **2022**, *12*, 1177, <https://doi.org/10.1038/s41598-022-05141-x>.
- [17] K. V. Kravchyk, H. Zhang, F. Okur, M. V. Kovalenko, *Acc. Mater. Res.* **2022**, *3*, 411, <https://doi.org/10.1021/accountsmr.2c00004>.
- [18] H. Koshikawa, S. Matsuda, K. Kamiya, M. Miyayama, Y. Kubo, K. Uosaki, K. Hashimoto, S. Nakanishi, *J. Power Sources* **2018**, *376*, 147, <https://doi.org/10.1016/j.jpowsour.2017.11.082>.
- [19] T. Krauskopf, H. Hartmann, W. G. Zeier, J. Janek, *ACS Appl. Mater. Interfaces* **2019**, *11*, 14463, <https://doi.org/10.1021/acsami.9b02537>.
- [20] M. Klimpel, H. Zhang, M. V. Kovalenko, K. V. Kravchyk, *Commun. Chem.* **2023**, *6*, 192, <https://doi.org/10.1038/s42004-023-01002-4>.
- [21] T. Fuchs, C. G. Haslam, F. H. Richter, J. Sakamoto, J. Janek, *Adv. Energy Mater.* **2023**, *13*, 2302383, <https://doi.org/10.1002/aenm.202302383>.
- [22] M. Klimpel, H. Zhang, G. Paggiaro, R. Dubey, F. Okur, L. P. H. Jeurgens, K. V. Kravchyk, M. V. Kovalenko, *Adv. Mater. Interfaces* **2024**, *11*, 2300948, <https://doi.org/10.1002/admi.202300948>.
- [23] W. Zaman, L. Zhao, T. Martin, X. Zhang, Z. Wang, Q. J. Wang, S. Harris, K. B. Hatzell, *ACS Appl. Mater. Interfaces* **2023**, *15*, 37401, <https://doi.org/10.1021/acsami.3c05886>.
- [24] S. Matsuda, K. Nakamura, *ACS Appl. Energy Mater.* **2020**, *3*, 11113, <https://doi.org/10.1021/acsaem.0c02085>.
- [25] M. J. Wang, R. Choudhury, J. Sakamoto, *Joule* **2019**, *3*, 2165, <https://doi.org/10.1016/j.joule.2019.06.017>.
- [26] K. Lee, E. Kazyak, M. J. Wang, N. P. Dasgupta, J. Sakamoto, *Joule* **2022**, *6*, 2547, <https://doi.org/10.1016/j.joule.2022.09.009>.
- [27] J.-M. Droux, H. Nguyen, D. H. S. Tan, A. Banerjee, X. Wang, E. A. Wu, C. Jo, H. Yang, Y. S. Meng, *Adv. Energy Mater.* **2020**, *10*, 1903253, <https://doi.org/10.1002/aenm.201903253>.

- [28] H. Zhang, F. Okur, C. Cancellieri, L. P. H. Jeurgens, A. Parrilli, D. T. Karabay, M. Nesvadba, S. Hwang, A. Neels, M. V. Kovalenko, K. V. Kravchyk, *Adv. Sci.* **2023**, *10*, 2205821, <https://doi.org/10.1002/advsc.202205821>.
- [29] F. Okur, H. Zhang, D. T. Karabay, K. Muench, A. Parrilli, A. Neels, W. Dachraoui, M. D. Rossell, C. Cancellieri, L. P. H. Jeurgens, K. V. Kravchyk, M. V. Kovalenko, *Adv. Energy Mater.* **2023**, *13*, 2203509, <https://doi.org/10.1002/aenm.202203509>.
- [30] H. Zhang, R. Dubey, M. Inniger, F. Okur, R. Wullich, A. Parrilli, D. T. Karabay, A. Neels, K. V. Kravchyk, M. V. Kovalenko, *Cell Rep. Phys. Sci.* **2023**, *4*, 101473, <https://doi.org/10.1016/j.xcrp.2023.101473>.
- [31] H. Zhang, F. Okur, B. Pant, M. Klimpel, S. Butenko, D. T. Karabay, A. Parrilli, A. Neels, Y. Cao, K. V. Kravchyk, M. V. Kovalenko, *ACS Appl. Mater. Interfaces.* **2024**, *16*, 12353, <https://doi.org/10.1021/acsami.3c14422>.
- [32] S. Afyon, K. V. Kravchyk, S. Wang, J. v. d. Broek, C. Hänsel, M. V. Kovalenko, J. L. M. Rupp, *J. Mater. Chem. A* **2019**, *7*, 21299, <http://doi.org/10.1039/C9TA04999A>.
- [33] K. V. Kravchyk, F. Okur, M. V. Kovalenko, *ACS Energy Lett.* **2021**, *6*, 2202, <https://doi.org/10.1021/acsenergylett.1c00672>.
- [34] H. Zhang, G. Paggiaro, F. Okur, J. Huwiler, C. Cancellieri, L. P. H. Jeurgens, D. Chernyshov, W. van Beek, M. V. Kovalenko, K. V. Kravchyk, *ACS Appl. Energy Mater.* **2023**, *6*, 6972, <https://doi.org/10.1021/acsaem.3c00459>.
- [35] H. Duan, F. Oluwatemitope, S. Wu, H. Zheng, Y. Zou, G. Li, Y. Wu, H. Liu, *ACS Appl. Mater. Interfaces.* **2020**, *12*, 52271, <https://doi.org/10.1021/acsami.0c16966>.
- [36] W. Xia, B. Xu, H. Duan, X. Tang, Y. Guo, H. Kang, H. Li, H. Liu, *J. Am. Ceram. Soc.* **2017**, *100*, 2832, <https://doi.org/10.1111/jace.14865>.
- [37] H. Liu, X.-B. Cheng, J.-Q. Huang, H. Yuan, Y. Lu, C. Yan, G.-L. Zhu, R. Xu, C.-Z. Zhao, L.-P. Hou, C. He, S. Kaskel, Q. Zhang, *ACS Energy Lett.* **2020**, *5*, 833, <https://doi.org/10.1021/acsenergylett.9b02660>.
- [38] G. V. Alexander, I. M. S. R. Murugan, *Ionics* **2021**, *27*, 4105, <https://doi.org/10.1007/s11581-021-04190-y>.
- [39] W. Jeong, S. S. Park, J. Yun, H. R. Shin, J. Moon, J.-W. Lee, *Energy Storage Mater.* **2023**, *54*, 543, <https://doi.org/10.1016/j.ensm.2022.10.044>.
- [40] R. Dubey, J. Sastre, C. Cancellieri, F. Okur, A. Forster, L. Pompizii, A. Priebe, Y. E. Romanyuk, L. P. H. Jeurgens, M. V. Kovalenko, K. V. Kravchyk, *Adv. Energy Mater.* **2021**, *11*, 2102086, <https://doi.org/10.1002/aenm.202102086>.
- [41] M.-C. Bay, M. Wang, R. Grissa, M. V. F. Heinz, J. Sakamoto, C. Battaglia, *Adv. Energy Mater.* **2020**, *10*, 1902899, <https://doi.org/10.1002/aenm.201902899>.
- [42] M.-C. Z. Bay, C. Battaglia, M. Wang, J. Sakamoto, US Patent Application No. US20210066747A1, **2021**.
- [43] R. Grissa, S. Payandeh, M. Heinz, C. Battaglia, *ACS Appl. Mater. Interfaces.* **2021**, *13*, 14700, <https://doi.org/10.1021/acsami.0c23144>.
- [44] R. Grissa, L. Seidl, W. Dachraoui, U. Sauter, C. Battaglia, *ACS Appl. Mater. Interfaces.* **2022**, *14*, 46001, <https://doi.org/10.1021/acsami.2c11375>.
- [45] M.-C. Bay, M. V. F. Heinz, R. Figi, C. Schreiner, D. Basso, N. Zanon, U. F. Vogt, C. Battaglia, *ACS Appl. Energy Mater.* **2019**, *2*, 687, <https://doi.org/10.1021/acsaem.8b01715>.
- [46] M. V. F. Heinz, M.-C. Bay, U. F. Vogt, C. Battaglia, *Acta Mater.* **2021**, *213*, 116940, <https://doi.org/10.1016/j.actamat.2021.116940>.
- [47] M.-C. Bay, M. V. F. Heinz, C. Linte, A. German, G. Blugan, C. Battaglia, U. F. Vogt, *Mater. Today Commun.* **2020**, *23*, 101118, <https://doi.org/10.1016/j.mtcomm.2020.101118>.
- [48] S. C. Ligon, G. Blugan, M.-C. Bay, C. Battaglia, M. V. F. Heinz, T. Graule, *Solid State Ion.* **2020**, *345*, 115169, <https://doi.org/10.1016/j.ssi.2019.115169>.
- [49] R. Grissa, C. Battaglia, US Patent Application No. US20230327191A1, **2023**.
- [50] M.-C. Bay, R. Grissa, K. V. Egorov, R. Asakura, C. Battaglia, *Mater. Futures* **2022**, *1*, 031001, <https://doi.org/10.1088/2752-5724/ac8947>.
- [51] S. C. Ligon, M.-C. Bay, M. V. F. Heinz, C. Battaglia, T. Graule, G. Blugan, *Materials* **2020**, *13*, 433, <https://doi.org/10.3390/ma13020433>.
- [52] L. Duchêne, R. S. Kühnel, D. Rentsch, A. Remhof, H. Hagemann, C. Battaglia, *Chem. Commun.* **2017**, *53*, 4195, <http://doi.org/10.1039/C7CC00794A>.
- [53] S. Payandeh, R. Asakura, P. Avramidou, D. Rentsch, Z. Łodziana, R. Černý, A. Remhof, C. Battaglia, *Chem. Mater.* **2020**, *32*, 1101, <https://doi.org/10.1021/acs.chemrev.0c00431>.
- [54] S. Payandeh, D. Rentsch, Z. Łodziana, R. Asakura, L. Bigler, R. Černý, C. Battaglia, A. Remhof, *Adv. Funct. Mater.* **2021**, *31*, 2010046, <https://doi.org/10.1002/adfm.202010046>.
- [55] A. Garcia, G. Müller, R. Černý, D. Rentsch, R. Asakura, C. Battaglia, A. Remhof, *J. Mater. Chem. A* **2023**, *11*, 18996, <http://dx.doi.org/10.1039/D3TA03914E>.
- [56] R. Asakura, A. Remhof, C. Battaglia, in 'Solid State Batteries Volume 1: Emerging Materials and Applications', Vol. 1413, American Chemical Society, **2022**, p. 353, <https://doi.org/10.1021/bk-2022-1413.ch014>.
- [57] R. Asakura, D. Reber, L. Duchêne, S. Payandeh, A. Remhof, H. Hagemann, C. Battaglia, *Energy Environ. Sci.* **2020**, *13*, 5048, <http://doi.org/10.1039/D0EE01569E>.
- [58] L. Duchêne, R. S. Kühnel, E. Stip, E. Cuervo Reyes, A. Remhof, H. Hagemann, C. Battaglia, *Energy Environ. Sci.* **2017**, *10*, 2609, <http://doi.org/10.1039/C7EE02420G>.
- [59] R. Asakura, L. Duchêne, S. Payandeh, D. Rentsch, H. Hagemann, C. Battaglia, A. Remhof, *ACS Appl. Mater. Interfaces* **2021**, *13*, 55319, <https://doi.org/10.1021/acsaami.1c15246>.
- [60] H. Braun, R. Asakura, A. Remhof, C. Battaglia, *ACS Energy Lett.* **2024**, *9*, 707, <https://doi.org/10.1021/acsenergylett.3c02117>.
- [61] A. Gigante, L. Duchêne, R. Moury, M. Pupier, A. Remhof, H. Hagemann, *ChemSusChem* **2019**, *12*, 4832, <https://doi.org/10.1002/cssc.201902152>.
- [62] L. Seidl, R. Grissa, L. Zhang, S. Trabesinger, C. Battaglia, *Adv. Mater. Interfaces* **2022**, *9*, 2100704, <https://doi.org/10.1002/admi.202100704>.
- [63] C. Fu, M. Jacob, Y. Sheima, C. Battaglia, L. Duchêne, L. Seidl, D. M. Opris, A. Remhof, *J. Mater. Chem. A* **2021**, *9*, 11794, <http://doi.org/10.1039/D1TA02689E>.
- [64] C. Fu, G. Homann, R. Grissa, D. Rentsch, W. Zhao, T. Gouveia, A. Falgayrat, R. Lin, S. Fantini, C. Battaglia, *Adv. Energy Mater.* **2022**, *12*, 2200412, <https://doi.org/10.1002/aenm.202200412>.
- [65] T. Schmaltz, F. Hartmann, T. Wicke, L. Weymann, C. Neef, J. Janek, *Adv. Energy Mater.* **2023**, *13*, 2301886, <https://doi.org/10.1002/aenm.202301886>.
- [66] F. Zhao, S. Zhang, Y. Li, X. Sun, *Small Struct.* **2022**, *3*, 2100146, <https://doi.org/10.1002/ssr.202100146>.
- [67] Y.-G. Lee, S. Fujiki, C. Jung, N. Suzuki, N. Yashiro, R. Omoda, D.-S. Ko, T. Shiratsuchi, T. Sugimoto, S. Ryu, J. H. Ku, T. Watanabe, Y. Park, Y. Aihara, D. Im, I. T. Han, *Nat. Energy* **2020**, *5*, 299, <https://doi.org/10.1038/s41560-020-0575-z>.
- [68] X. Wu, C. Villeveille, P. Novák, M. El Kazzi, *J. Mater. Chem. A* **2020**, *8*, 5138, <https://doi.org/10.1039/c9ta14147b>.
- [69] X. Wu, M. Mirolo, C. A. F. Vaz, P. Novák, M. El Kazzi, *ACS Appl. Mater. Interfaces.* **2021**, *13*, 42670, <https://doi.org/10.1021/acsami.1c09605>.
- [70] W. Z. Huang, C. Z. Zhao, P. Wu, H. Yuan, W. E. Feng, Z. Y. Liu, Y. Lu, S. Sun, Z. H. Fu, J. K. Hu, S. J. Yang, J. Q. Huang, Q. Zhang, *Adv. Energy Mater.* **2022**, *12*, 2201044, <https://dx.doi.org/10.1002/aenm.202201044>.
- [71] X. Wu, M. El Kazzi, C. Villeveille, *J. Electroceram.* **2017**, *38*, 207, <https://doi.org/10.1007/s10832-017-0084-z>.
- [72] L. Höltzsch, F. Jud, C. Borca, T. Huthwelker, C. Villeveille, V. Pelé, C. Jordy, M. El Kazzi, P. Novák, *J. Electrochem. Soc.* **2020**, *167*, 110558, <https://dx.doi.org/10.1149/1945-7111/aba36f>.
- [73] X. Wu, PhD Eidgenössische Technische Hochschule 25999, Zürich, **2019**, <https://doi.org/10.3929/ethz-b-000352747>.
- [74] M. Mirolo, PhD Eidgenössische Technische Hochschule 27215, Zürich, **2020**, <https://doi.org/10.3929/ethz-b-000479623>.
- [75] L. Höltzsch, PhD Eidgenössische Technische Hochschule 27931, Zürich, **2021**, <https://doi.org/10.3929/ethz-b-000547149>.
- [76] L. Höltzsch, C. Borca, T. Huthwelker, F. Marone, C. M. Schlepütz, V. Pelé, C. Jordy, C. Villeveille, M. El Kazzi, P. Novák, *Electrochim. Acta* **2021**, *389*, 138735, <https://doi.org/10.1016/j.electacta.2021.138735>.
- [77] X. Wu, C. Villeveille, P. Novák, M. El Kazzi, *Phys. Chem. Chem. Phys.* **2018**, *20*, 11123, <https://doi.org/10.1039/c8cp01213j>.
- [78] M. Mirolo, X. Wu, C. A. F. Vaz, P. Novák, M. El Kazzi, *ACS Appl. Mater. Interfaces.* **2021**, *13*, 2547, <https://doi.org/10.1021/acsami.0c17936>.
- [79] M. Mirolo, D. Leanza, L. Höltzsch, C. Jordy, V. Pelé, P. Novák, M. El Kazzi, C. A. F. Vaz, *Anal. Chem.* **2020**, *92*, 3023, <https://doi.org/10.1021/acs.analchem.9b04124>.
- [80] X. Wu, J. Billaud, I. Jerjen, F. Marone, Y. Ishihara, M. Adachi, Y. Adachi, C. Villeveille, Y. Kato, *Adv. Energy Mater.* **2019**, *9*, 1901547, <https://doi.org/10.1002/aenm.201901547>.
- [81] S. P. Culver, R. Koerver, W. G. Zeier, J. Janek, *Adv. Energy Mater.* **2019**, *9*, 1900626, <https://doi.org/10.1002/aenm.201900626>.
- [82] A. Stefancic, M. El Kazzi, US Patent Application No. US20230299263A1, **2023**.
- [83] N. J. Dudney, *Electrochem. Soc. Interface* **2008**, *17*, 44, <https://doi.org/10.1149/2.F04083IF>.
- [84] A. Aribia, J. Sastre, X. Chen, E. Gilshtein, M. H. Futscher, A. N. Tiwari, Y. E. Romanyuk, *J. Electrochem. Soc.* **2021**, *168*, 040513, <https://doi.org/10.1149/1945-7111/abf215>.
- [85] M. Fehse, R. Trócoli, E. Ventosa, E. Hernández, A. Sepúlveda, A. Morata, A. Tarancón, *ACS Appl. Mater. Interfaces.* **2017**, *9*, 5295, <https://doi.org/10.1021/acsami.6b15258>.
- [86] J. Li, C. Ma, M. Chi, C. Liang, N. J. Dudney, *Adv. Energy Mater.* **2015**, *5*, 1401408, <https://doi.org/10.1002/aenm.201401408>.
- [87] A. Aribia, J. Sastre, X. Chen, M. H. Futscher, M. Rumpel, A. Priebe, M. Döbeli, N. Osenciat, A. N. Tiwari, Y. E. Romanyuk, *Adv. Energy Mater.* **2022**, *12*, 2201750, <https://doi.org/10.1002/aenm.202201750>.

- [88] M. H. Futscher, L. Brinkman, A. Müller, J. Casella, A. Aribia, Y. E. Romanyuk, *Commun. Chem.* **2023**, *6*, 110, <https://doi.org/10.1038/s42004-023-00901-w>.
- [89] J. Sastre, X. Chen, A. Aribia, A. N. Tiwari, Y. E. Romanyuk, *ACS Appl. Mater. Interfaces*. **2020**, *12*, 36196, <https://doi.org/10.1021/acsami.0c09777>.
- [90] J. Casella, J. Morzy, E. Gilshtein, M. Yarema, M. H. Futscher, Y. E. Romanyuk, *ACS Nano* **2024**, *18*, 4352, <https://doi.org/10.1021/acsnano.3c10146>.
- [91] X. Chen, J. Sastre, A. Aribia, E. Gilshtein, Y. E. Romanyuk, *ACS Appl. Energy Mater.* **2021**, *4*, 5408, <https://doi.org/10.1021/acsaem.1c01283>.
- [92] J. Sastre, A. Priebe, M. Döbeli, J. Michler, A. N. Tiwari, Y. E. Romanyuk, *Adv. Mater. Interfaces* **2020**, *7*, 2000425, <https://doi.org/10.1002/admi.202000425>.
- [93] A. Müller, F. Okur, A. Aribia, N. Osenciat, C. A. F. Vaz, V. Siller, M. El Kazzi, E. Gilshtein, M. H. Futscher, K. V. Kravchyk, M. V. Kovalenko, Y. E. Romanyuk, *Mater. Adv.* **2023**, *4*, 2138, <http://doi.org/10.1039/D3MA00155E>.
- [94] J. Sastre, M. H. Futscher, L. Pompizi, A. Aribia, A. Priebe, J. Overbeck, M. Stiefel, A. N. Tiwari, Y. E. Romanyuk, *Commun. Mater.* **2021**, *2*, 76, <https://doi.org/10.1038/s43246-021-00177-4>.
- [95] M. H. Futscher, T. Amelal, J. Sastre, A. Müller, J. Patidar, A. Aribia, K. Thorwarth, S. Siol, Y. E. Romanyuk, *J. Mater. Chem. A* **2022**, *10*, 15535, <http://doi.org/10.1039/D2TA02843C>.
- [96] A. Müller, L. Paravicini, J. Morzy, M. Krause, J. Casella, N. Osenciat, M. H. Futscher, Y. E. Romanyuk, *ACS Appl. Mater. Interfaces* **2024**, *16*, 695, <https://doi.org/10.1021/acsami.3c14693>.
- [97] J. Schnell, T. Günther, T. Knoche, C. Vieider, L. Köhler, A. Just, M. Keller, S. Passerini, G. Reinhart, *J. Power Sources* **2018**, *382*, 160, <https://doi.org/10.1016/j.jpowsour.2018.02.062>.
- [98] M. Vilkmann, M. Ylikunnari, O. Sorsa, A. Laukkanen, D. Urishov, S. Malburet, Y. Nait Abdi, M. Maréchal, S. Sadki, P. Rannou, in 'Norbatt2022', Goteborg, Sweden, **2022**.
- [99] <https://hidden-project.eu/>
- [100] P. Iurilli, L. Luppi, C. Brivio, *Energies* **2022**, *15*, 6904, <https://doi.org/10.3390/en15196904>.
- [101] L. Pires Da Veiga, S. Sharad Bhoir, D. Brüllmann, S. Malburet, S. Müller, M. Stalder, C. Brivio, A. Ingenito, *Batter. Supercaps* **2024**, <https://doi.org/10.1002/batt.202300591>.
- [102] <https://thesolidproject.eu/>.

#### License and Terms



This is an Open Access article under the terms of the Creative Commons Attribution License CC BY 4.0. The material may not be used for commercial purposes.

The license is subject to the CHIMIA terms and conditions: (<https://chimia.ch/chimia/about>).

The definitive version of this article is the electronic one that can be found at <https://doi.org/10.2533/chimia.2024.403>